Efficient optimisation of a vehicle suspension system, using a gradient-based approximation method. Part 1. Mathematical modelling

M.J. Thoresson*, P.E. Uys*, P.S. Els[1,*], J.A. Snyman*
12 May 2009

Abstract—A methodology is proposed for the efficient determination of gradient information, when performing gradient based optimisation of an off-road vehicle's suspension system. The methodology is applied to a computationally expensive, non-linear vehicle model, that exhibits severe numerical noise. A recreational off-road vehicle is modelled in MSC.ADAMS, and coupled to MATLAB for the execution of the optimisation. The successive approximation method, Dynamic-Q, is used for the optimisation of the spring and damper characteristics. Optimisation is performed for both ride comfort and handling. The determination of the objective function value is performed using computationally expensive numerical simulations.

This paper proposes a non-linear pitch-plane model, to be used for the gradient information, when optimising ride comfort. When optimising for handling, a non-linear four wheel model, that includes roll, is used. The gradients of the objective function and constraint functions are obtained through the use of central finite differences, within Dynamic-Q, via numerical simulation using the proposed simplified models. The importance of correctly scaling these simplified models is emphasised. The models are validated against experimental results. The simplified vehicle models exhibit significantly less numerical noise than the full vehicle simulation model, and solve in significantly less computational time.

Keywords— Dynamic-Q, gradient-based mathematical optimisation, semi-active, ride comfort, handling, vehicle suspension.

1. INTRODUCTION

The use of mathematical optimisation techniques for the improvement of the engineering design process is rapidly gaining acceptance. There is great debate in the optimisation world as to whether gradient based approximation techniques or stochastic based methods, like genetic algorithms, are more efficient and suited to engineering design. Stochastic techniques generally require a large starting population, in order to achieve a sufficiently feasible solution. This makes the

[1]Address correspondance to: Schalk Els, Tel.: +27 12 420 2045; Fax: +27 12 362 5087; E-mail: schalk.els@up.ac.za; web page: www.me.up.ac.za
*Department of Mechanical and Aeronautical Engineering, University of Pretoria, Pretoria 0002, South Africa.

stochastic methods computationally expensive, when expensive numerical models, of the physical system are to be optimised. Most researchers have to utilise costly multiple processing systems, as the desktop computer can take days or even weeks to arrive at a solution. On the other hand, gradient based optimisation techniques tend to be heavily dependent on the initial starting point, and require accurate gradient information for the iterative approximation of the design space. The determination of this gradient information, is costly when many design variables are considered. The gradient calculation is also adversely affected by numerical noise that is normally inherent in complex numerical simulation models, e.g. full vehicle models. Research, with reference to vehicle suspension optimisation, is now briefly discussed.

Dahlberg [1, 2], as early as 1977, investigated the optimisation of a vehicle's suspension system for ride comfort and working space, subject to a random road input. A 1-degree of freedom (dof) model, was optimised using the Sequential Unconstrained Minimisation Technique (SUMT). This was then expanded to a linear 2-dof model, to investigate the speed dependence of the optimal suspension settings. It was found that for a small suspension working space the optimal spring and damper settings are heavily dependent on vehicle speed, while for a large working space the optimum is not really dependant on vehicle speed. It is suggested that active suspension systems be considered when small suspension working spaces are available.

Eberhard, Bestle and Piram [3] successfully used gradient based optimisation methods (a sequential quadratic programming, or SQP, algorithm) to optimise a simple pitch-plane vehicle model's non-linear damper characteristics for ride comfort. The non-linear damper characteristic is modelled with piecewise Hermite splines. The Hermite splines, however, require difficult to handle constraints in order to ensure feasibility of the optimised damper characteristic. Nevertheless, satisfactory results were obtained. Boggs and Tolle [4] provide an introduction to the SQP method and discuss recent developments.

Etman et. al. [5] designed a stroke dependent damper, for the front axle of a truck, using Sequential Linear Programming (SLP), a gradient based optimisation algorithm. They use a 2-dof quarter car model, for the initial investigation of the desired non-linear damper characteristics. Ride comfort is optimised using discrete road obstacles. The non-linear damper characteristics are modelled using an empirical piecewise quadratic approximation. Finally a full vehicle model is used for the ride comfort optimisation, for one discrete road obstacle. Bump-stop contact is ignored, to remove numerical noise and lessen computational expense. Difficulties were experienced due to poor finite difference approximations of the gradients, and with multiple feasible optima being found.

Naudé and Snyman [6, 7] and Naudé [8] make use of a pitch-plane vehicle model to optimise the piecewise linear damper characteristics of an off-road military vehicle, for ride comfort. The 'Leap-Frog' (LFOPC) optimisation algorithm [9] was used, and although taking many iterations to reach the optimum, the optimisation was complete

within a few seconds, because the vehicle model was specially written for the vehicle being investigated.

Baumal, McPhee and Calamai [10] compared the efficiency of a Genetic Algorithm (GA) to a gradient-based optimisation method (gradient projection method) for a pitch-plane vehicle model, that was computationally efficient. The GA converged to an optimum that was only a 4% improvement over the gradient based method, but, required thousands more objective function evaluations.

Eberhard, Schiehlen and Bestle [11] investigate the use of a stochastic optimiser (simulated annealing) and a gradient-based (deterministic) optimiser (a SQP algorithm) for the optimisation of a full linear vehicle model's ride comfort. The four design variables considered are the linear spring and damper coefficients, the distance of the body center of gravity (cg) between the axles and the track width of the wheels. They conclude that deterministic optimisation approaches offer rapidly converging algorithms, that often get stuck in local minima when optimising multi-body dynamic systems. Nevertheless, the global optimum may be obtained by these methods if used within a multi-start strategy. They also find that simulated annealing is useful in avoiding local minima. It does, however, require substantially more function evaluations in order to locate the global optimum. Thus both methods are successful in locating the global optimum. They consequently suggest a hybrid combination of stochastic and deterministic algorithms for optimisation. They state, however, that the switching strategy is and will continue to be a challenging task.

Eriksson and Friberg [12] optimised the linear spring and damper characteristics of the engine mounting system on a city bus, for ride comfort. Use was made of a linear finite element method (FEM) model to simulate the response of the bus to a given road input, with three passenger positions used for the ride comfort objective function. Only a 7 % improvement in ride comfort was achieved and it was found that the local minima, to which the gradient based algorithm (form of SQP algorithm, with gradients determined by forward finite differencing) converged to, were heavily dependent on the initial starting point. Eriksson and Arora [13] investigated the use of three continuous global optimisation methods for the ride comfort optimisation of the city bus. It was found that the modified zooming method in terms of number of objective function evaluations (464) is most efficient in locating the global optimum.

Gobbi, Mastinu and Doniselli [14] and Gobbi et. al. [15] use a back-propagated Artificial Neural Network (ANN) of the full vehicle simulation model, coupled with a genetic algorithm for the optimisation of ride and handling of a sedan vehicle. Suspension non-linearities are modelled as piecewise linear approximations. The full simulation model has been verified against test data. The ANN was used for function evaluations within the genetic algorithm optimisation process. However, this methodology requires an extensive number of function evaluations, of the expensive full simulation model, to sufficiently train a representative ANN, making it infeasible for stand-alone workstations.

Schuller, Haque and Eckel [16] optimised the comfort and handling of a BMW sedan using a simplified vehicle model composed of transfer functions. Because of the nature of the vehicle model the design parameters were allowed to have a small variance of 15% over the current vehicle design. This process thus aims to refine an already feasible design for the next model launch. The numerical model solves faster than real-time, making the use of genetic algorithms feasible. Only open loop handling manœuvres were considered for the optimisation process.

Andersson and Eriksson [17] optimised the non-linear damper and spring characteristics of a full city bus vehicle model, that was validated against test data. The model consists of non-linear bushings, bump-stops, springs, dampers and a non-linear 'Magic Formula' tyre model. The ride comfort of the bus was optimised for three discrete road obstacles, with a 23 % improvement achieved. The handling was optimised using a single lane change manœuvre at 40 and 80 km/h, with a 6 % improvement achieved. The handling objective function is defined as a combination of the yaw rate gain and yaw rate time lag, with an inequality constraint limiting the maximum body roll angle to less than 1.3 $degrees$. The built-in MSC.ADAMS SQP method was used, and the optima were reached after approximately 145 function evaluations. An attempt was made at the combined optimisation of handling and ride comfort, and it was found that the result is heavily dependent on the weights assigned to the various performance objectives.

Els et. al. [18] compared the efficiency of the Dynamic-Q optimisation algorithm to the SQP method for vehicle suspension optimisation. They found that the use of central finite differencing for the determination of gradient information improved the convergence of the Dynamic-Q optimisation algorithm towards a feasible optimum within fewer objective function evaluations, when compared to SQP or Dynamic-Q with forward finite differencing. The objective functions exhibited severe noise. It appeared, however, that using central finite differencing with relatively large steps in computing gradient information, was successful in smoothing out the effect of the noise in the optimisation.

Bandler et. al. [19] and Koziel, Bandler and Madsen [20] introduced to the engineering optimisation world the theory of 'Space Mapping', which makes use of a coarse simple model (surrogate model) and a detailed fine model for the optimisation process. The Space Mapping technique involves the matching and updating of the coarse model to more accurately describe the fine model. This has been used successfully for the structural optimisation of a vehicle for crash safety, by Redhe and Nilsson [21]. In their research the coarse model was constructed using linear Response Surface Methodology (RSM) with the optimisation converging within 14 iterations, and using a total of 26 expensive function evaluations. However, the RSM model must be trained.

The concept of Automatic Differentiation (AD) is a novel way of obtaining gradient information with one function evaluation [22, 23]. This methodology was evaluated by

Bischof et. al. [24] for the shape optimisation of an airfoil, with the objective function being evaluated by a software chain. Although AD provides more accurate gradient information than forward finite differences, the evaluation of the objective function was approximately 16 times slower than the original code for eight ($n = 8$) design variables. Using forward finite differences would have used the original code $n + 1$ times, equating to a cost of nine times the cost of one function evaluation of the original code. The other downside of AD is that access to the original source code is necessary, and it is normally not available when commercial simulation software, such as MSC.ADAMS is used.

The research, described in the current paper, proposes the use of carefully chosen simplified numerical models of the vehicle dynamics for computing gradient information, and a detailed vehicle model for obtaining objective function values at each iteration step. This allows for the more efficient use of gradient approximation methods for optimisation. This paper discusses the vehicle models and the optimisation algorithm used.

A case study for the optimisation of an off-road vehicle's spring and damper characteristics for ride comfort and handling is presented. The vehicle is fitted with a '4-State Semi-Active Suspension System' ($4S_4$) [25] currently under development. The vehicle is modelled using a full non-linear MSC.ADAMS model, including non-linear suspension and tyre characteristics.

2. OPTIMISATION PROCEDURE

The gradient-based optimisation algorithm, Dynamic-Q [26], using central finite difference approximations for the gradients, is used for the current research. The Dynamic-Q method has been developed to address the general optimisation problem:

$$\underset{w.r.t.\mathbf{x}}{minimize} \quad f(\mathbf{x}), \;\; \mathbf{x} = [x_1, x_2, .., x_n]^T \in R^n \tag{1}$$

subject to the inequality constraints:

$$g_j(\mathbf{x}) \leq 0, \;\; j = 1, 2, .., m \tag{2}$$

and the equality constraints:

$$h_j(\mathbf{x}) = 0, \;\; j = 1, 2, .., r \tag{3}$$

where $f(\mathbf{x})$, $g_j(\mathbf{x})$ and $h_j(\mathbf{x})$ are scalar functions of $\mathbf{x}$. In this formulation $\mathbf{x}$ is the vector of design variables, $f(\mathbf{x})$ is the objective function, $g_j(\mathbf{x})$ the inequality constraint functions, and $h_j(\mathbf{x})$ the equality constraint functions.

The Dynamic-Q algorithm is defined as: 'Applying a *Dynamic* trajectory optimisation algorithm to successive spherical *Quadratic* approximations of the actual optimisation problem' [26]. This algorithm has the major advantage that it requires

relatively few function evaluations (simulations) of the original expensive objective and constraint functions to construct simple quadratic approximate functions. These new functions can then be evaluated cheaply and the optimum point of the associated approximate optimisation sub-problem may be found economically, using the robust dynamic trajectory method LFOPC [9]. At this new approximate optimum point, a new quadratic approximate optimisation sub-problem is constructed, that is again solved. This procedure is iteratively repeated until convergence is obtained. This method is very efficient for optimising objective functions that require an expensive computer simulation for their evaluation. The details of the method can be found in the publications by Snyman and Hay [26], and Els and Uys [27] where it was applied to a similar vehicle as in this study.

In this research simplified numerical models of the full vehicle model, are used for the determination of gradient information. Although the Dynamic-Q optimisation method is used, the principle can be applied to any gradient-based optimisation method. For the determination of the required first order gradient information central finite differencing is used. Central finite differencing was found to significantly improve the gradient based optimisation process by Thoresson [28] and Els et. al. [18]. The use of the simplified vehicle models for the determination of the gradient information, reduces the number of numerically expensive simulations of the full vehicle model to one per iteration, as it is only required to obtain the objective and constraint function values. This has the advantage that the total optimisation time is greatly reduced, as the analysis of the simplified models take approximately 10% of the simulation time of the full vehicle model. Traditionally the use of central finite differences would have resulted in $2n + 1$ full simulations per iteration, where n is the number of design variables. In this case the optimisation takes effectively, in terms of computational time, $2n$ times 0.1 for the gradient and 1 for the objective function resulting in $0.2n + 1$ function evaluations per iteration.

3. VEHICLE SUSPENSION UNIT

The suspension unit currently under development, has the unique feature that it incorporates two damper packs (fitted with bypass valves) and two gas accumulators, effectively giving two damper characteristics and two spring characteristics in a single suspension unit. This unit will be refered to as the ‘4-State Semi-Active Suspension System’, or $4S_4$ [25]. Switching between the two spring and damper characteristics is achieved by solenoid valves as illustrated in Figure 1. Valve switching times vary between 50 and 100 milliseconds depending on system pressure. Spring and damper characteristics can be taken as design variables, to be optimised for both ride comfort and handling respectively. It is assumed that the suspension system will switch between the ride comfort and handling option, to suite the operating

conditions. Provided an intelligent control system can distinguish between the two different operating conditions, and switch the suspension system to the correct setting. Each operating setting is expected to have different optimum values for the spring and damper characteristics. This suspension has the ability to eliminate the traditional ride comfort vs. handling compromise.

4. FULL VEHICLE MODEL

A Land Rover Defender 110 is modelled in MSC.ADAMS View [29] with standard suspension settings, as a baseline. The non-linear MSC.ADAMS Pacejka 89 tyre model [30] is fitted to measured tyre data, and used within the model. The tyre's vertical dynamics and load dependent lateral dynamics are considered in this model. In order to keep the model as simple as possible, yet as complex as necessary, longitudinal dynamic behaviour of the tyres and vehicle is not considered here. The vehicle body is modelled as two rigid bodies connected along the roll axis at the chassis height, by a revolute joint and a torsional spring, in order to better capture the vehicle dynamics due to body torsion in roll. The anti-roll bar is modelled as a torsional spring between the two rear trailing arms to be representative of the actual anti-roll bar's effect. The bump and rebound stops, are modelled with non-linear splines, as force elements between the axles and vehicle body. The suspension bushings are modelled as kinematic joints with torsional spring characteristics that are representative of the actual vehicle's suspension joint characteristics, in an effort to speed up the solution time, and help decrease numerical noise. The baseline vehicle's springs and dampers are modelled with measured non-linear splines. The vehicle's center of gravity (cg) height and moments of inertia were measured [31] and used within the model. Only the spring and damper characteristics are changed for optimisation purposes. The $4S_4$ unit has been included in the MSC.ADAMS model, using the MSC.ADAMS Controls environment to include the Simulink model, and replaces the standard springs and dampers. Figure 2 indicates the detailed kinematic modelling of the rear and front suspensions. The complete model consists of 15 unconstrained degrees of freedom, 16 moving parts, 6 spherical joints, 8 revolute joints, 7 Hooke's joints, and one motion defined by the steering driver. The degrees of freedom are:

Body	Degrees of Freedom	Associated Motions
Vehicle Body	7	body torsion
(2 rigid bodies)		longitudinal, lateral, vertical
		roll, pitch, yaw
Front Axle	2	roll, vertical
Rear Axle	2	roll, vertical
Wheels	4 x 1	rotation

The vehicle's direction of heading is controlled by a carefully tuned yaw rate steering driver, adjusting the front wheels' steering angles according to the difference of the desired course from the current course at a preview distance ahead of the vehicle.

The longitudinal driver is modelled as a variable force attached to the body at wheel height depending on the difference between the instantaneous speed and desired speed. This MSC.ADAMS model is linked to MATLAB [32] through a Simulink block that requires as inputs the spring and damper design variable values, and returns outputs of vertical accelerations, vehicle body roll angle and roll velocity.

4.1. Validation of Full Vehicle Model

The MSC.ADAMS full vehicle model is validated against measured results, from physical tests performed on the baseline vehicle. The correlation results are presented in Figure 3 for the baseline vehicle travelling over two discrete bumps to evaluate vertical dynamics, and in Figure 4 for the vehicle performing a double lane change manœuvre at 65 km/h. From the results it is evident that the model returns excellent correlation to the actual vehicle. It is, however, computationally expensive to solve and exhibits severe numerical noise with respect to the design variables defined in Section 5, due to all the included non-linear effects.

5. DEFINITION OF OPTIMISATION PARAMETERS

5.1. Definition of Design Variables

In choosing the design variables for optimisation, the assumption is made that the left and right suspension settings will be the same, but that front and rear settings may differ. The design variables chosen for optimisation are therefore the static gas volume of the accumulator (Figure 5), and damper force scale factor (Figure 6), on both the front and rear axles. Thus there are two design variables per axle.

For this initial study the standard rear damper force characteristic is multiplied by a factor which constitutes the damping design variable (Figure 6). The general shape and switch velocities of the damper are thus kept the same. This paper only considers the cases of two and four design variables, which respectively corresponds to the case where the spring and damper characteristics are identical for the front and rear axles (two design variables), and where they may differ for front and rear (four design variables).

The static gas volume of the accumulator is denoted by $gvol$, and allowed to range from 0.1 to 0.6 $liters$. The range is dictated by the smallest and largest gas volumes that are possible with the current $4S_4$ unit. The damper force scale factor is denoted by $dpsf$, and allowed to range from 0.1 to 3. The range is again determined by the

current design limits of the $4S_4$ unit. The design variables are normalised to allow a range from 0.001 to 1 in magnitude, which are accordingly chosen as upper and lower bounds. The normalisation of the design variables is generally sound optimisation practice, to ensure that the problem to be solved by the optimisation algorithm, is not poorly scaled. Poor scaling results in optimisation difficulties, and poor convergence. The i^{th} design variable x_i is defined as a ratio of: the parameter's current value $v_{_{current}}$, the lowest permissible value $v_{_{low}}$, and the highest permissible value $v_{_{high}}$, as follows:

$$x_i = \frac{v_{_{current}} - v_{_{low}}}{v_{_{high}} - v_{_{low}}} \tag{4}$$

The design variables are then explicitly defined as follows:

$$x_1 = \tfrac{dpsf-0.1}{3-0.1}, \;\; x_2 = \tfrac{gvol-0.1}{0.6-0.1} \tag{5}$$

with bounds

$$0.001 \leq x_i \leq 1, \;\; i = 1, 2 \tag{6}$$

For the four design variable problem the front and rear settings are uncoupled. This means that there are separate front and rear damper scale factors and front and rear spring static gas volumes. This results in two design variables describing the front and two describing the rear, giving four design variables in total.

The front damper scale factor is denoted by $dpsf$, the front static gas volume by $gvolf$, the rear damper scale factor by $dpsfr$, and the rear static gas volume by $gvolr$. These design variables are also allowed to range from 0.001 to 1 in magnitude. Thus the design variables are defined explicitly as follows:

$$\begin{aligned} x_1 &= \tfrac{dpsff-0.1}{3-0.1}, \;\; x_2 = \tfrac{gvolf-0.1}{0.6-0.1} \\ x_3 &= \tfrac{dpsfr-0.1}{3-0.1}, \;\; x_4 = \tfrac{gvolr-0.1}{0.6-0.1} \end{aligned} \tag{7}$$

with bounds

$$0.001 \leq x_i \leq 1, \;\; i = 1, ..., 4 \tag{8}$$

5.2. Definition of Objective Functions

For ride comfort the motion of the vehicle is simulated for travelling in a straight line over the local Belgian paving, and the sum of the driver a_{zRMSd} and passenger a_{zRMSp} frequency weighted (according to British Standard 6841 [33]) root mean square (RMS) vertical accelerations are used for the objective function. This was found to be a sufficiently representative measure of passengers' subjective comments by Els [34]. The Belgian paving test track used, is located at the Gerotek Test Facilities

[35], and has a ISO8608 [36] roughness coefficient G_{do} of $1 \times 10^{-4}\ m^2/(cycles/m)$, and a terrain index ω of 4 [28]. Following sound optimisation practice the objective function is scaled as for the design variables to range between zero and one (equations 5 to 8). This is done by assuming that the maximum and minimum objective function values will lie on one of the corners of the design space. The four corners for the two design variable case were evaluated. The maximum vertical RMS acceleration was found to be 4.4 m/s^2, and the minimum to be 0.7 m/s^2. RMS accelerations are then scaled so that the expected maximum and minimum values lie between zero and one. The ride comfort objective function $f_{ride}(x)$, is defined as the sum of the scaled driver and passenger accelerations divided by two, as follows:

$$f_{ride}(x) = \frac{\sum(\frac{a_{zRMSd}-0.7}{4.4-0.7}, \frac{a_{zRMSp}-0.7}{4.4-0.7})}{2} \tag{9}$$

The motion sickness component is ignored as the track is not long enough to evaluate such low frequencies. In a study by Griffin et. al. [37], it was found that the motion sickness component is more dependent on individual driver style than on the vehicle's suspension system.

The handling objective function is defined as the sum of the normalised first peak value of the body roll angle $\varphi_{1^{st}peak}$ for the first lane change [27] of the ISO3888 [38] double lane change manœuvre, and the normalised RMS roll velocity $\dot{\varphi}_{RMS}$ for the whole double lane change manœuvre. The roll angle was found to be a suitable metric of vehicle handling by Uys et. al. [39]. The RMS roll velocity is used in addition to the roll angle, so as to have a measure of the transient stability of the vehicle in roll. The handling objective function $f_{hand}(x)$ is defined as the sum of these normalised parameters divided by two, as follows:

$$f_{hand}(x) = \frac{\sum(\frac{(\dot{\varphi}_{RMS}-0.8)0.9}{5.7-0.8} + 0.1, \frac{(\varphi_{1^{st}peak}-1.4)0.9}{12.2-1.4} + 0.1)}{2} \tag{10}$$

5.3. Definition of Inequality Constraint Functions

Tyre hop effects need to be considered when optimising for ride comfort, as the damping design variables tend to be sensitive to tyre hop. The requirement was introduced, that the tyre could only be permitted to loose contact with the ground for 10% or less of the simulation time, when considering typical off-road and rough terrain as used in this investigation. The time the tyre has lost contact with the ground was determined by observing when the tyre's vertical force F_{ztyre_i} is equal to zero. The tyre hop effect is added as inequality constraints for each individual tyre i as follows:

$$g_i(x) = 10(\frac{\sum t(F_{ztyre_i} = 0)}{t_{total}} - 0.1) \leq 0 \tag{11}$$

The factor of 10 was used to better scale the tyre hop constraint between minus one and one.

6. SIMPLIFIED VEHICLE MODELS

The need for simplified smoother models to obtain gradient information, is justified by the high amplitude noise inherently present in the MSC.ADAMS simulation model, as illustrated in Figure 7. This figure reflects the change in the ride comfort objective function value for a change in only the front damper design variable x_1. This was performed at the center of the design space. It can be seen that the noise in relation to the objective function value is severe, especially when considering the tyre hop constraint values. Figure 8 represents the objective and constraint values for changes in the front damper design variable, for the simplified vehicle model. It can be seen that the noise present in the objective function is greatly reduced, although no significant benefit is observed when considering the constraint functions. It is speculated, that this is attributed to the low tyre damping, which results in unstable tyre dynamics.

6.1. Handling Model

For the simplified vehicle handling model it is assumed that the vehicle drives on a smooth surface, and uses exactly the same steering input as the MSC.ADAMS model for that iteration. The model consists of two parts, first the lateral and yaw dynamics, and then the resulting roll dynamics of the body. For the formulation of the equations of motion for the simplified handling model, Figures 9 and 10 are considered. The model is simplified so that only three degrees of freedom are considered, namely: body roll θ, vehicle yaw ψ and vehicle lateral displacement y. The assumption will be made that the vehicle will drive at a constant longitudinal velocity $\dot{x}$ along the vehicle's x-axis. Looking at the top view of the vehicle (Figure 9) the overall yaw and lateral equations of motion can be formulated. For yaw:

$$\sum M_z = I_z\ddot{\psi} = a(F_{y1} + F_{y2}) - b(F_{y3} + F_{y4}) \tag{12}$$

where it is assumed that the steer angle δ is small (i.e. $F_{yi}cos(\delta) \approx F_{yi}$). Thus the full lateral tyre force F_{yi} acts along the y-axis. Also the longitudinal component of the lateral tyre force is low in magnitude and can be ignored. For the lateral direction:

$$\sum F_y = m_v\ddot{y_v} = F_{y1} + F_{y2} + F_{y3} + F_{y4} \tag{13}$$

Similarly by considering Figure 10 the equation of motion for the body roll about the body cg can be formulated as follows:

$$\sum M_x = I_x\ddot{\varphi} = (f_{4S_{4l}} - f_{4S_{4r}})\frac{t_s}{2} + h_{cg}(F_{yl} + F_{yr})\frac{m_b}{m_v} \tag{14}$$

Where m_v is the entire vehicle mass (i.e. $m_b + m_a$, see Figure 10). The mass ratio $\frac{m_b}{m_v}$ is introduced so that the the tyres' lateral force effect on the vehicle body can be uncoupled from the axles and wheels, as the body motion is what our suspension can control. This was done so as to decrease the number of degrees of freedom to be calculated, helping to speed up simulation time. The left $f_{4S_{4l}}$ and right $f_{4S_{4r}}$ suspension forces are the sum of the suspension forces on the respective side. Similarly the left F_{yl} and right F_{yr} lateral forces are the sum of the lateral tyre forces for the respective side. The lateral forces are calculated by taking the vertical load and slip angle for the tyre, as inputs to the 'Magic Formula' Pacejka'89 [30] tyre model using the same coefficients as for the full vehicle simulation model. For this model the following simplifications have been applied:

- The tyre lateral force produces a minimal longitudinal component that is taken up by the longitudinal driving force and can be ignored.
- No longitudinal effects except vehicle speed are considered.
- Nothing can be done about the tyre deflection and the angle that the axle makes with respect to the ground.
- For this reason the axle roll effects, due to tyre deflection are ignored.
- The MSC.ADAMS calculated tyre slip angles are used as the input slip angles for the MATLAB simulation.
- Vertical tyre forces are taken as being the same mass proportion front to rear as the static case, of the side suspension force.

The simplified handling model is thus a significant simplification of the actual vehicle dynamics. It will be shown to still return very good trends when compared to the full vehicle simulation model.

6.2. Ride Comfort Model

For the simplified ride comfort vehicle model a simple pitch plane vehicle model is used, similar to that used by Eberhard et al, Etman et al, Naudé et al [3, 5, 6] and many others. The measured rough road profile seen by the full vehicle model's wheels is averaged left and right to give an effective centerline profile. The pitch plane model then follows the averaged path using a point follower tyre model. The basic layout of the simplified model is indicated in Figure 11. The equations describing the vehicle behaviour are derived as follows. Consider the forces acting on the front unsprung

mass m_{tf}, as a result of the road disturbance input z_{rf}. The summation of vertical forces on the unsprung masses leads to:

$$\sum F_z = m_{tf}\ddot{z_3} = 2k_{tf}(-z_3 + z_{rf} + \delta_{stat}) + 2c_{tf}(-\dot{z_3} + \dot{z_{rf}}) - m_{tf}g - 2f_{4S_{4f}} \tag{15}$$

for the front, and similarly for the rear:

$$\sum F_z = m_{tr}\ddot{z_4} = 2k_{tr}(-z_4 + z_{rr} + \delta_{stat}) + 2c_{tr}(-\dot{z_4} + \dot{z_{rr}}) - m_{tr}g - 2f_{4S_{4r}} \tag{16}$$

where the 2 relates to the fact that there is both a left and a right $4S_4$ strut. It is taken that $g = 9.81m/s^2$. The m_{tf} is the total front axle unsprung mass including the two tyres. And $f_{4S_{4f}}$ is the $4S_4$ front suspension force which is a function of the displacement of the vehicle body m_b and the unsprung mass:

$$f_{4S_{4f}} = f(z_3 - z_1 + \theta a, \dot{z_3} - \dot{z_1} + \dot{\theta}a) \tag{17}$$

The rear suspension force $f_{4S_{4r}}$ can similarly be defined as:

$$f_{4S_{4r}} = f(z_4 - z_1 - \theta b, \dot{z_4} - \dot{z_1} - \dot{\theta}b) \tag{18}$$

The tyre spring stiffness and damping are only active while the tyre is in contact with the ground thus the following if statement also applies:

$$\begin{array}{ccc} if\ z_3 - z_{rf} - \delta_{stat} < 0 & & \\ then & k_{tf} = k_t & c_{tf} = c_t \\ else & k_{tf} = 0 & c_{tf} = 0 \end{array} \tag{19}$$

For the sprung mass m_b two equations of motion are applicable, first for vertical motion:

$$\sum F_z = m_b\ddot{z_1} = m_bg - 2f_{4S_{4f}} - 2f_{4S_{4r}} \tag{20}$$

and then for pitch motion:

$$\sum M_y = I_y\ddot{\theta} = a2f_{4S_{4f}} - b2f_{4S_{4r}} \tag{21}$$

These equations of motion can be manipulated as follows:

$$\begin{array}{c} -m_b\ddot{z_1} = -m_bg + 2f_{4S_{4f}} + 2f_{4S_{4r}} \\ -I_y\ddot{\theta} = -a2f_{4S_{4f}} + b2f_{4S_{4r}} \\ m_{tf}\ddot{z_3} + 2k_{tf}z_3 + 2c_{tf}\dot{z_3} = 2k_{tf}(z_{rf} + \delta_{stat}) + 2c_{tf}\dot{z_{rf}} - m_{tf}g - 2f_{4S_{4f}} \\ m_{tr}\ddot{z_4} + 2k_{tr}z_4 + 2c_{tr}\dot{z_4} = 2k_{tr}(z_{rr} + \delta_{stat}) + 2c_{tr}\dot{z_{rr}} - m_{tr}g - 2f_{4S_{4r}} \end{array} \tag{22}$$

This results in a clear set of matrices for mass $\mathbf{M}$, stiffness $\mathbf{K}$, damping $\mathbf{C}$, and force F, which correspond with the formula:

$$\mathbf{M}\ddot{z} + \mathbf{K}z + \mathbf{C}\dot{z} = F \tag{23}$$

The above differential equations can be re-arranged, in order to be solved with a numerical integration scheme, as follows:

$$\begin{Bmatrix} \dot{z} \\ \ddot{z} \end{Bmatrix} = \begin{bmatrix} \mathbf{O} & \mathbf{I} \\ -\mathbf{M}^{-1}\mathbf{K} & -\mathbf{M}^{-1}\mathbf{C} \end{bmatrix} \begin{Bmatrix} z \\ \dot{z} \end{Bmatrix} + \begin{Bmatrix} O \\ \mathbf{M}^{-1}F \end{Bmatrix} \tag{24}$$

The modelling units of the models are meters and radians. For the execution of the numerical integration of the simplified models, the built-in MATLAB ode45 [32], Runge-Kutta solver is used with a relative tolerance of 1.5 mm/s^2 and a maximum time step of 0.05 seconds.

6.3. Validation of Simplified Models

6.3.1. Handling Model Validation

Figures 12 and 13 illustrate the comparison between the full vehicle MSC.ADAMS model and the simplified model for the handling objective function parameters. It can be seen that the simplified model does not capture all the information of the full vehicle model. Although the the minimums and maximums are not numerically the same, they occur in approximately the same position in the design space. In general the trends are very similar, while only varying in absolute values. The MATLAB handling model is thus scaled so as to give a better approximation of the MSC.ADAMS full vehicle model. For the scaling of the MATLAB simplified models, the two design variables were considered and 30 function evaluations were performed over the design space using the full MSC.ADAMS simulation model and the simplified model. The results for the simplified model were then scaled so that the surfaces coincided over most of the design space. This was achieved by considering the current Matlab function value $F_{Mcurrent}$, the maximum Matlab function value F_{Mmax}, and the minimum Matlab function value F_{Mmin}, the maximum ADAMS function value F_{Amax}, and minimum ADAMS function value F_{Amin}. The simplified model function value F_s used for the determination of gradient information will thus be defined as follows:

$$F_s = \frac{(F_{Mcurrent} - F_{Mmin})(F_{Amax} - F_{Amin})}{(F_{Mmax} - F_{Mmin})} + F_{Amin} \tag{25}$$

6.3.2. Ride Model Validation

The simplified MATLAB model for ride comfort was evaluated against the full MSC.ADAMS vehicle model to investigate whether the gradient closely matched that of the MSC.ADAMS model. The sum of the vertical weighted accelerations was normalised in both cases so that the objective function value would range from zero

to one. Figures 14 to 16 illustrate the close correlation achieved when observing the effect of the design parameters on the objective function and the tyre hop effect. Again numerical values are not the same but the trends are very similar.

7. CONCLUSIONS

This paper proposes the combined use of simplified numerical vehicle models and computationally expensive full vehicle simulation models in gradient-based optimisation algorithms, for vehicle suspension optimisation.

In particular the specific optimisation methodology to be used is described and the objective functions and design variables are defined. The full vehicle is modelled in MSC.ADAMS. This model is validated against measured test results with excellent correlation being achieved. However, this model is computationally expensive and exhibits severe numerical noise.

In order to help overcome the problems associated with high computational cost and numerical noise in the optimisation process, simplified models of the vehicle are described. These models exhibit very similar trends to the full vehicle simulation model, however, the absolute values are not the same. It is also important to note that the constraints, especially the tyre hop constraints, do not necessarily cross the zero axis at the correct points, even though the gradient trends are very similar. The required scaling of the simplified models to be more representative of the full vehicle model is presented. The cost of this scaling must be taken into account when optimising. Here 30 expensive full vehicle model simulations per simplified model were performed. The simplified model's objective functions were suitably scaled, to be representative of the full simulation model's objective function values. Once scaled, the simplified models are representative of the full vehicle simulation model, but exhibit significantly less numerical noise, and solve significantly faster.

Part 2 of this paper investigates the implementation of the simplified models in the optimisation procedure. The optimisation results using the full simulation vehicle model throughout, will be compared with that obtained using the simplified models for computation of the gradient information.

ACKNOWLEDGEMENTS

- Optimisation related investigations were performed under the auspices of the Multi-disciplinary Design Optimisation Group (MDOG) of the Department of Mechanical and Aeronautical Engineering of the University of Pretoria, and the National Research Foundation (NRF) under Thutuka Contract No. TTK-2004-081-0000-43.

- The vehicle dynamics simulation for the design of the controllable suspension system is based upon work supported by the European Research Office of the US Army under Contract's N68171-01-M-5852, N62558-02-M-6372 and N62558-04-P-6004.

REFERENCES

1. Dahlberg, T.: Parametric Optimisation of a 1-DOF Vehicle Travelling on a Randomly Profiled Road. *Journal of Sound and Vibration* 55, 2 (1977), pp. 245–253.
2. Dahlberg, T.: An Optimised Speed Controlled Suspension of a 2-DOF Vehicle Travelling on a Randomly Profiled Road. *Journal of Sound and Vibration* 64, 4 (1979), pp. 541–546.
3. Eberhard, P., Bestle, D., Piram, U.: Optimisation of Damping Characteristics in non-linear Dynamic Systems. *First World Congress of Structural and Multidisiciplinary Optimisation* (1995), pp. 863–870.
4. Boggs, P.T., Tolle, J.W.: Sequential Quadratic Programming for Large-Scale Non-Linear Optimisation. *Journal of Computational and Applied Mathematics* 124 (2000), pp. 123–137.
5. Etman, L.F.P., Vermeulen, R.C.N., van Heck, J.G.A.M., Schoofs, A.J.G., van Campen, D.H.: Design of a Stroke Dependent Damper for the Front Axle Suspension of a Truck Using Multibody System Dynamics and Numerical Optimisation. *Vehicle System Dynamics* 38 (2002), pp. 85–101.
6. Naudé, A.F., Snyman, J.A.: Optimisation of Road Vehicle Passive Suspension Systems. Part 1. Optimisation Algorithm and Vehicle Model. *Applied Mathematical Modelling* 27 (2003), pp. 249–261.
7. Naudé, A.F., Snyman, J.A.: Optimisation of Road Vehicle Passive Suspension Systems. Part 2. Qualification and Case Study. *Applied Mathematical Modelling* 27 (2003), pp. 263–274.
8. Naudé, A.F.: Computer Aided Design Optimisation of Road Vehicle Suspension Systems, PhD Thesis. *University of Pretoria, South Africa* (2001). http://upetd.up.ac.za/thesis/available/etd-06202008-160123/unrestricted/00front.pdf accessed on 11/05/2009.
9. Snyman, J.A.: The LFOPC Leap-Frog Algorithm for Constrained Optimisation. *Computers and Mathematics with Applications* 40, pp. 1085–1096 (2000).
10. Baumal, A.E., McPhee, J., Calamai, P.H.: Application of Genetic Algorithms to the Optimisation of an Active Vehicle Suspension Design. *Computer Methods in Applied Mechanics and Engineering* 163 (1998), pp. 87–94.
11. Eberhard, P., Schiehlen, W., Bestle, D.: Some Advantages of Stochastic Methods in Multicriteria Optimisation of Multibody Systems. *Archive of Applied Mechanics* 69 (1999), pp. 543–554.
12. Eriksson, P., Friberg, O.: Ride Comfort Optimisation of a City Bus. *Structural and Multidisciplinary Optimisation* 20 (2000), pp. 67–75.
13. Eriksson, P., Arora, J.S.: Comparison of Global Optimisation Algorithms Applied to a Ride Comfort Optimisation Problem. *Structural and Multidisciplinary Optimisation* 24 (2002), pp. 157–167.
14. Gobbi, M., Mastinu, G., Doniselli, C.: Optimising a Car Chassis. *Vehicle System Dynamics* 32 (1999), pp. 149–170.
15. Gobbi, M., Mastinu, G., Doniselli, C., Guglielmetto, L., Pisino, E.: Optimal and Robust Design of a Road Vehicle Suspension System. *Vehicle System Dynamics Supplement* 33 (1999), pp. 3–22.
16. Schuller, J., Haque, I., Eckel, M.: An Approach for Optimisation of Vehicle Handling Behaviour in Simulation. *Vehicle System Dynamics Supplement* 37 (2002), pp. 24–37.
17. Andersson, D., Eriksson, P.: Handling and Ride Comfort Optimisation of an Inter-city Bus. *Vehicle System Dynamics Supplement* 41 (2004), pp. 547–556.
18. Els, P.S., Uys, P.E., Snyman, J.A., Thoresson, M.J.: Gradient-Based Approximation Methods Applied to

the Optimal Design of Vehicle Suspension Systems Using Computational Models with Severe Inherent Noise. *Mathematical and Computer Modelling* 43-7/8 (2006), pp. 787–801.
19. Bandler, J.W., Cheng, Q.S., Dakroury, S.A., Mohamed, A.S., Bakr, M.H., Madsen, K., Søndergaard, J.: Space Mapping: The State of the Art. *IEEE Transactions on Microwave Theory and Techniques* 52-1, 337–361 (2004).
20. Koziel, S., Bandler, J.W., Madsen, K.: Towards a Rigorous Formulation of the Space Mapping Technique for Engineering Design. *Circuits and Systems* ISCAS 2005 IEEE International Symposium, 5605–5608 (23-26 May 2005).
21. Redhe, M., Nilsson, L.: Optimisation of the new Saab 9-3 exposed to impact load using a space mapping technique. *Structural and Multidisciplinary Optimisation* 27, 411–420 (2004).
22. Tolsma, J.E., Barton, P.I.: On Computational Differentiation. *Computers in Chemical Engineering* 22-4/5, 475–490 (1998).
23. Bartholomew-Biggs, M., Brown, S., Christianson, B., Dixon, L.: Automatic Differentiation of Algorithms. *Journal of Computational and Applied Mathematics* 124, 171–190 (2000).
24. Bischof, C.H., Bücker, H.M., Lang, B., Rasch, A., Slusanschi, E.: Efficient and Accurate Derivatives for a Software Process Chain in Airfoil Shape Optimisation. *Future Generation Computer Systems* 21, 1333–1344 (2005).
25. Theron, N.J., Els, P.S.: Modelling of a semi-active hydropneumatic spring-damper unit. *International Journal of Vehicle Design* 45/4, 501–521 (2007).
26. Snyman, J.A., Hay, A.M.: The Dynamic-Q Optimisation Method: An Alternative to SQP? *Computers and Mathematics with Applications* 44, 1589–1598 (2002).
27. Els, P.S., Uys, P.E.: Investigation of the Applicability of the Dynamic-Q Optimisation Algorithm to Vehicle Suspension Design. *Mathematical and Computer Modeling* 37 (2003), pp. 1029–1046.
28. Thoresson, M.J.: Mathematical Optimisation of the Suspension System of an Off-Road Vehicle for Ride comfort and Handling, MEng Thesis. *University of Pretoria, South Africa* (2003). http://upetd.up.ac.za/thesis/available/etd-11162005-155118/unrestricted/00dissertation.pdf accessed on 11/05/2009.
29. Getting Started Using MSC.ADAMS View, Version 2005. *MSC Corporation* (2005).
30. Bakker, E., Pacejka, H.B., Linder, L.: A New Tire Model with an Application in Vehicle Dynamics Studies. *SAE 890087*.
31. Uys, P.E., Els, P.S., Thoresson, M.J., Voigt, K.G., Combrink, W.C.: Experimental determination of moments of inertia for an off-road vehicle in a regular engineering laboratory. *International Journal of Mechanical Engineering Education* 34/4, 291–314 (2005).
32. MATLAB Release 12 Users guide. *Mathworks* (2000).
33. British Standards Institution: British Standard Guide to Measurement and Evaluation of Human Exposure to Whole-Body Mechanical Vibration and Repeated Shock. *BS6841* (1987).
34. Els, P.S.: The Applicability of Ride Comfort Standards to Off-Road Vehicles. *Journal of Terramechanics* 42-1 (2005), pp. 47–64.
35. Gerotek Test Facility, South Africa, www.gerotek.co.za *accessed 10 April 2006.*
36. The International Organisation for Standardisation: Mechanical Vibration - Road Surface Profiles - Reporting of Measured Data. *ISO 8608* (01 September 1995).
37. Griffin, M.J., Newman, M.M.: An Experimental Study of Low-Frequency Motion in Cars. *Proceedings of the Institute of Mechanical Engineers, Part D: Journal of Automotive Engineering* 218, 1231–1238 (2004).
38. The International Organisation for Standardisation: Passenger Cars - Test Track for a Severe Lane-Change Manœuvre - Part 1: Double Lane-Change. *ISO 3888-1* (06 October 2004).
39. Uys, P.E., Els, P.S., Thoresson, M.J.: Criteria for Handling Measurement. *Journal of Terramechanics* 43-1 (2006), pp. 43–67.

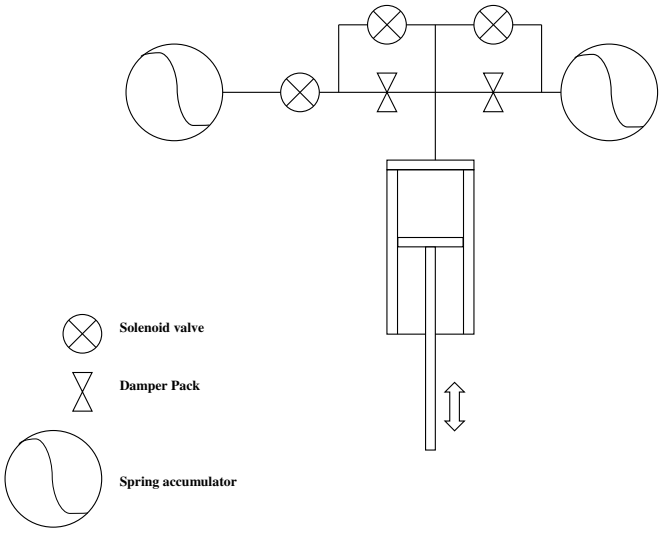

Fig. 1. $4S_4$ Suspension Unit

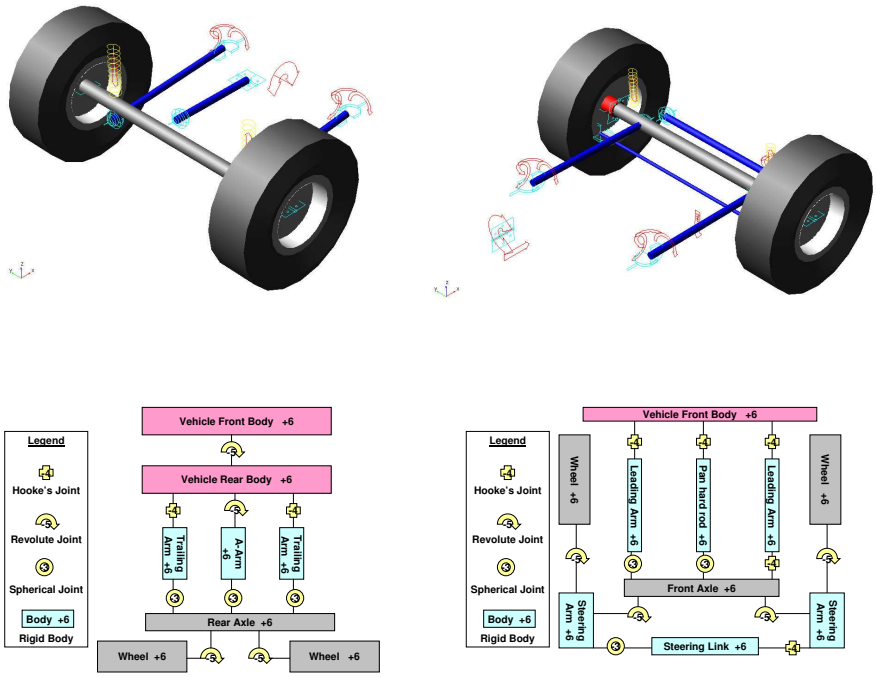

Fig. 2. Modelling of the rear and front suspensions in MSC.ADAMS

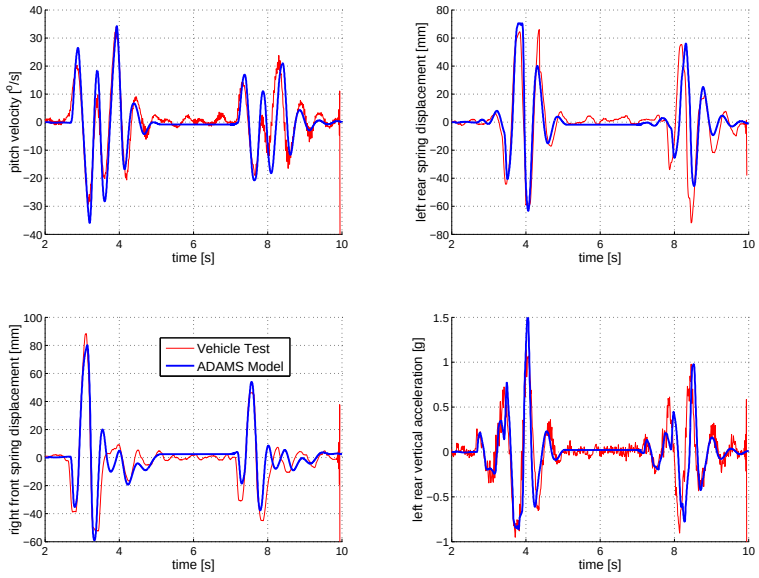

Fig. 3. Discrete bumps, 15 km/h, validation of MSC.ADAMS Model's vertical dynamics

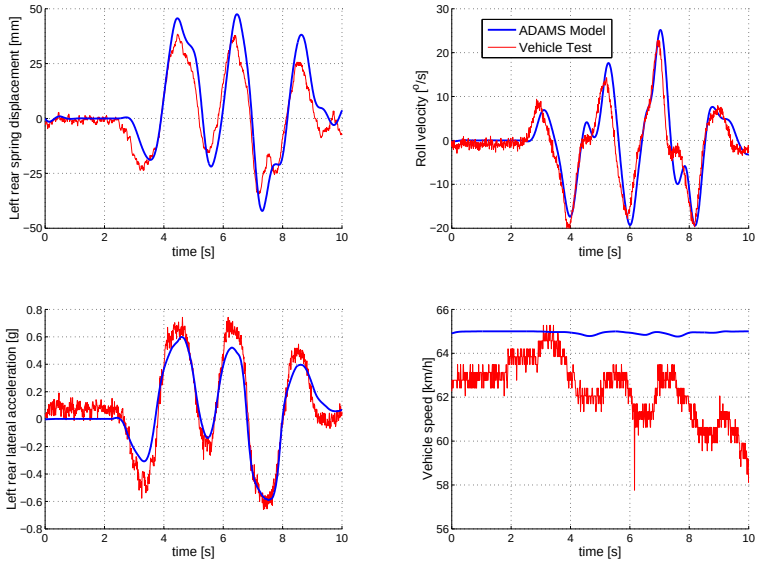

Fig. 4. Double lane change, 65 km/h, validation of MSC.ADAMS model's handling dynamics

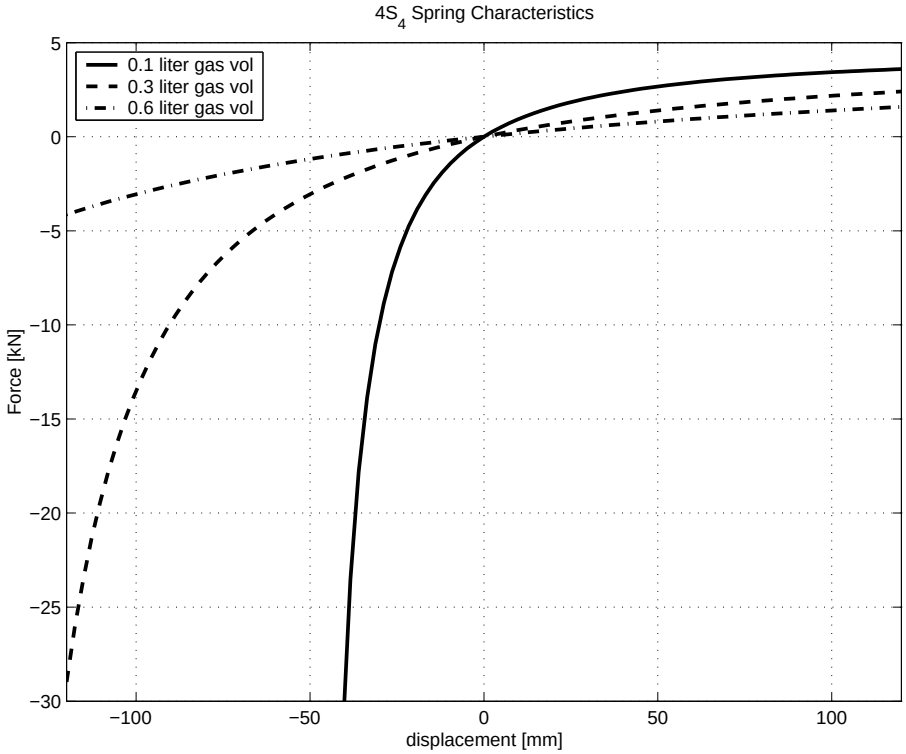

Fig. 5. Definition of $4S_4$ Spring characteristics for various gas volumes

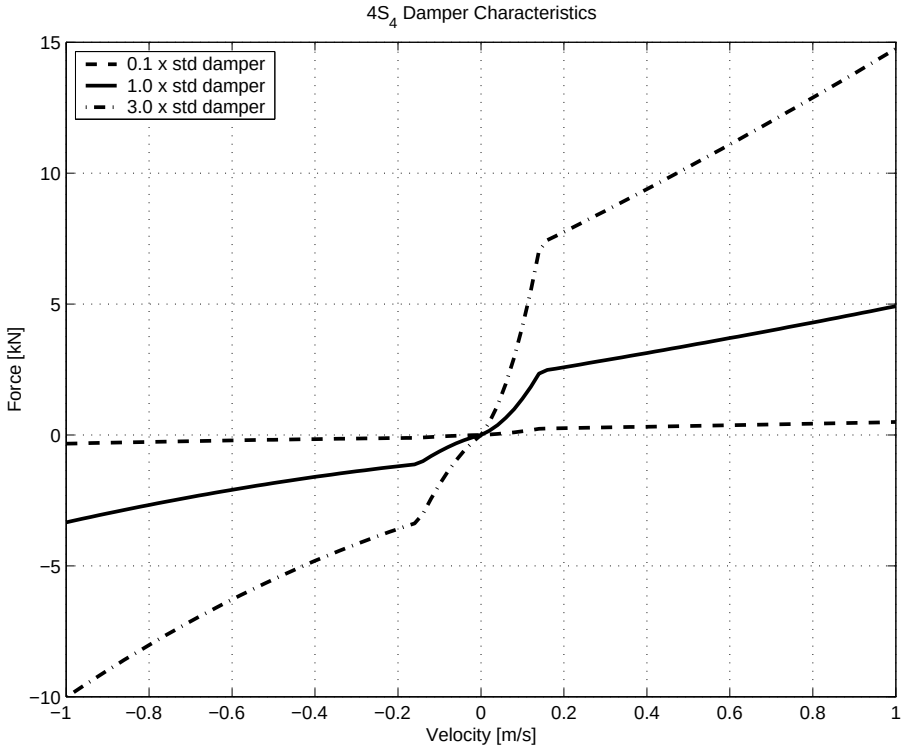

Fig. 6. Definition of $4S_4$ damper characteristics for various damper scale factors

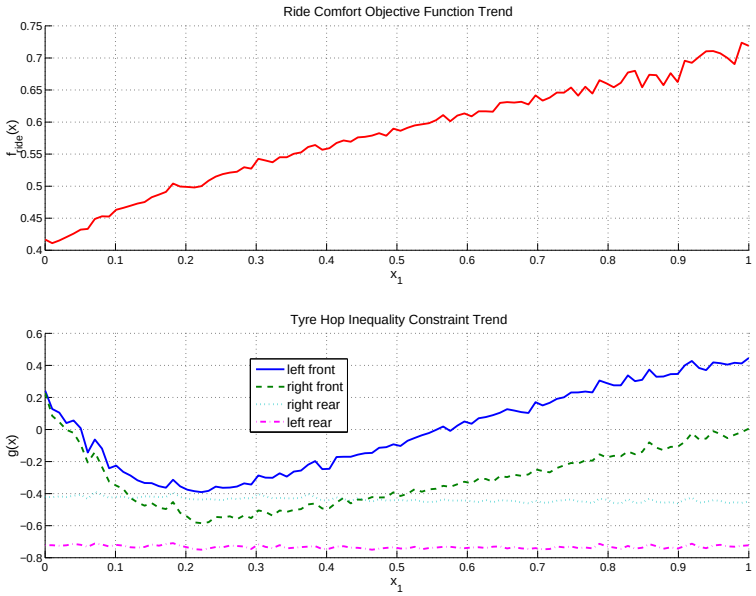

Fig. 7. Level of inherent numerical noise in objective function and inequality constraints, for change in front damper design variable x_1, for full vehicle MSC.ADAMS model

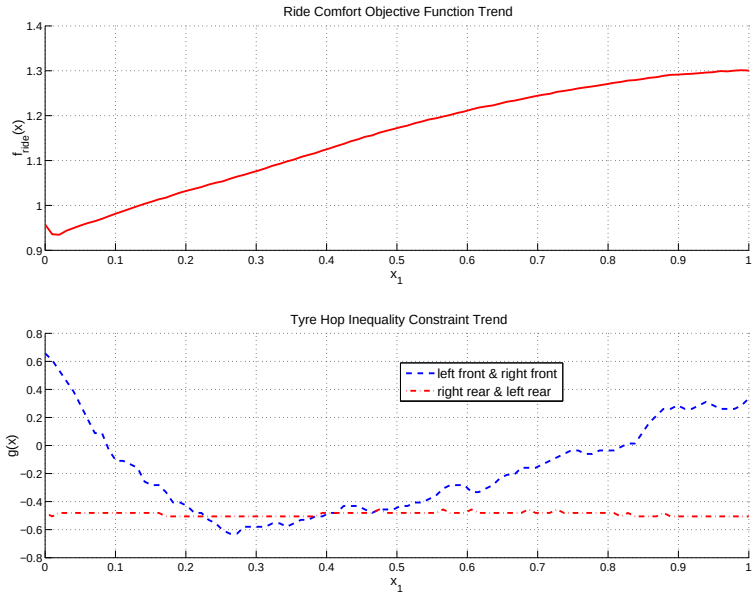

Fig. 8. Level of inherent numerical noise in objective function and inequality constraints, for change in front damper design variable x_1, when considering the simplified MATLAB model

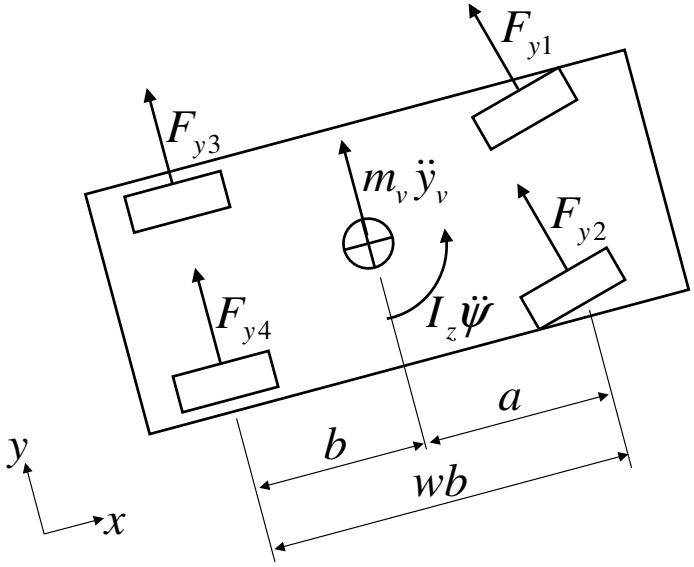

Fig. 9. Top View of vehicle in handling manœuvre

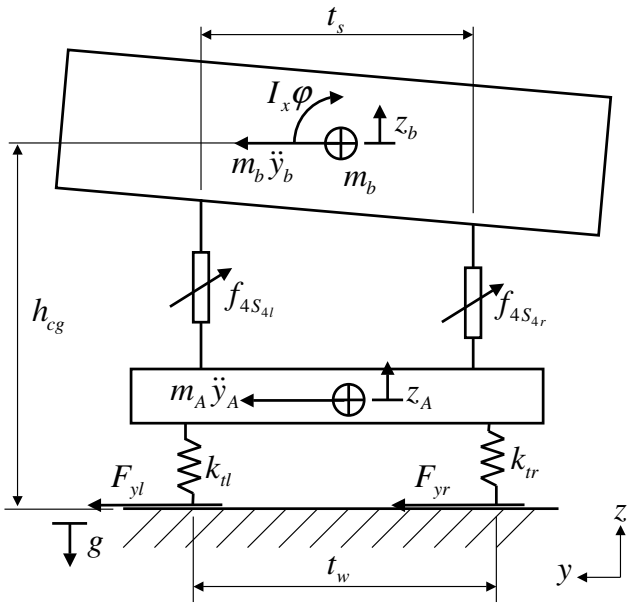

Fig. 10. Rear view of vehicle indicating body roll

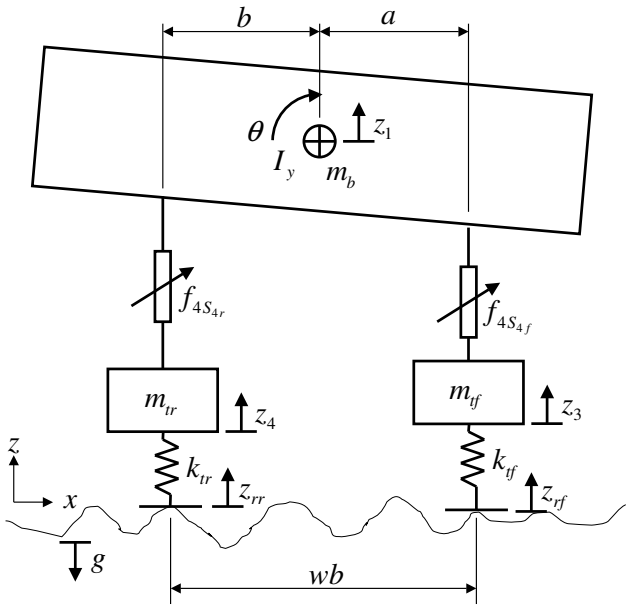

Fig. 11. Simple pitch-plane vehicle model

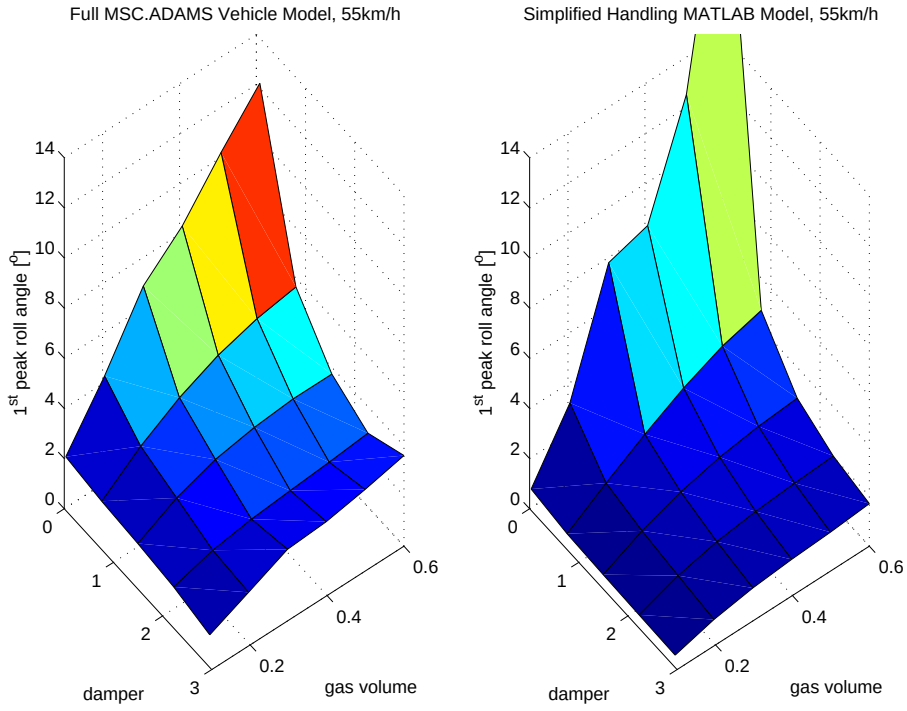

Fig. 12. Validation of 1st peak roll angle over design space, for double lane change.

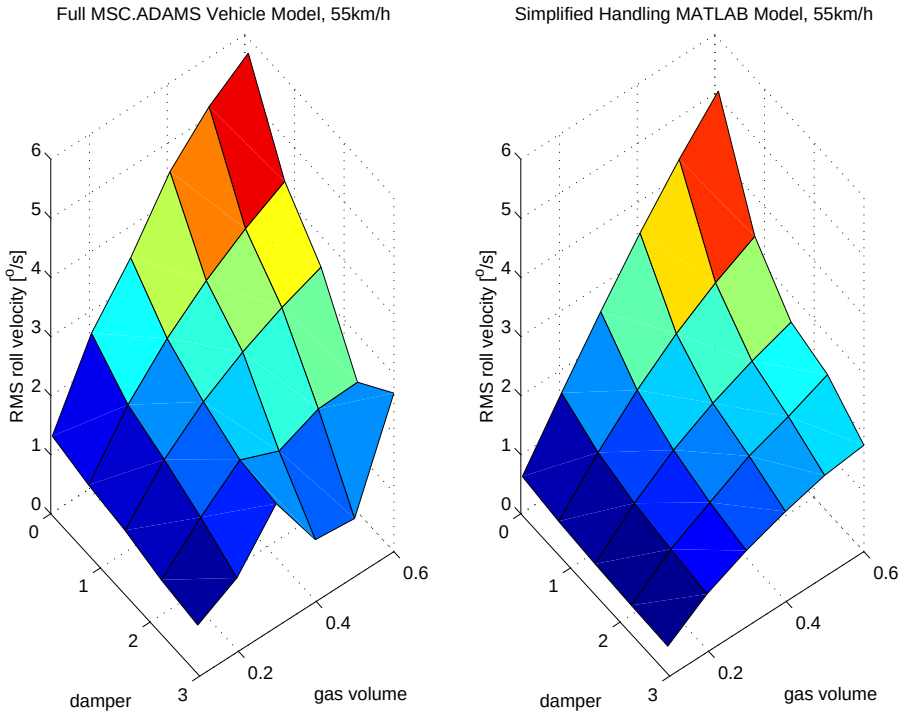

Fig. 13. Validation of RMS roll velocity over design space, for double lane change.

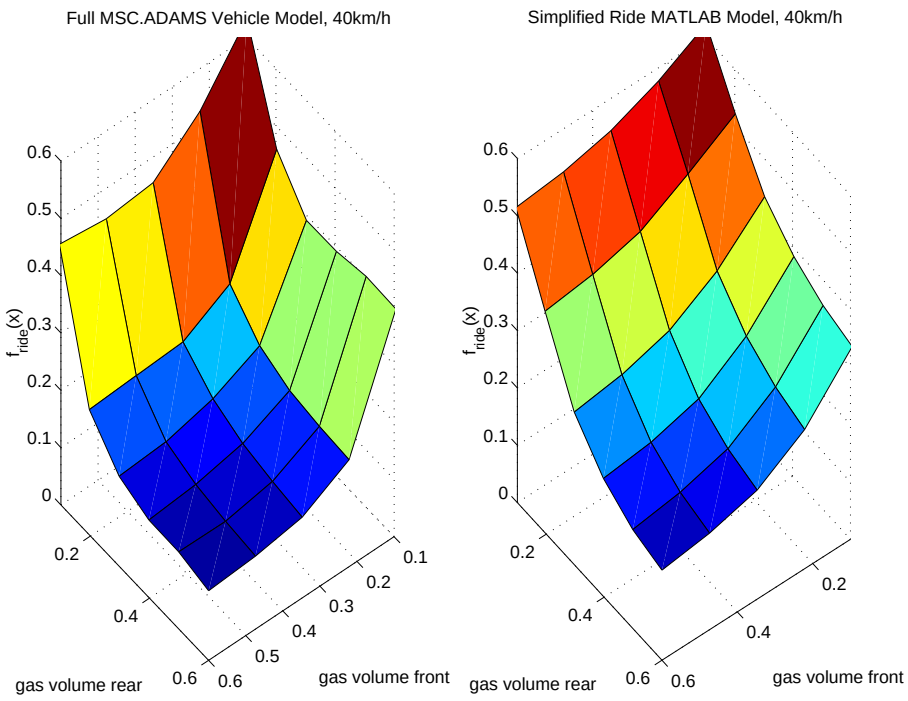

Fig. 14. Model validation of ride comfort for differing front and rear gas volumes

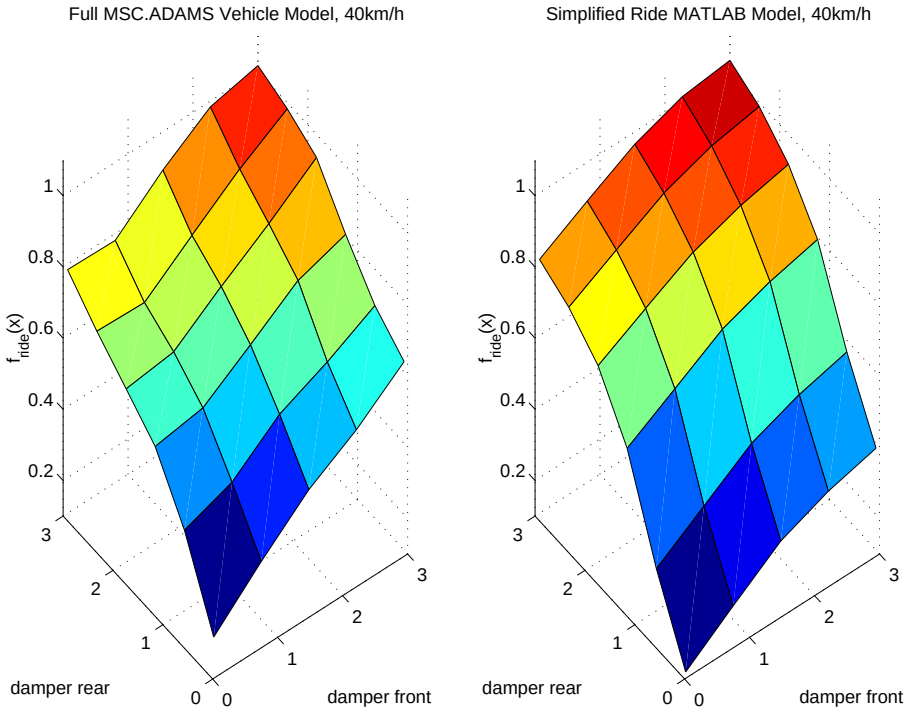

Fig. 15. Model validation of ride comfort for differing front and rear damper scale factors

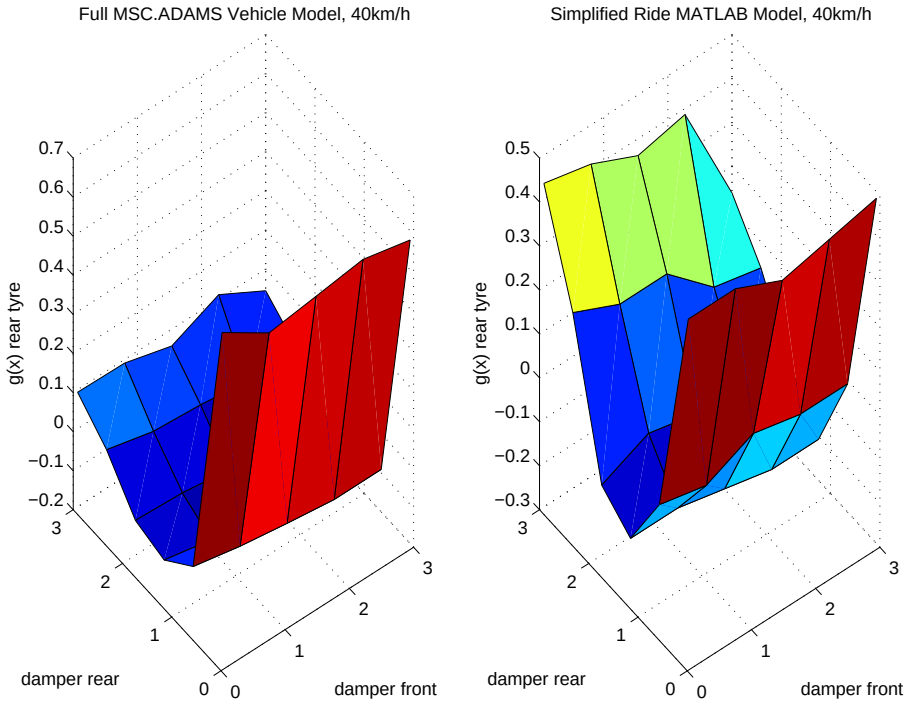

Fig. 16. Model validation of ride comfort for differing front and rear damper scale factors: effect on rear tyre hop